Isolation of a methyl-reducing methanogen outside the Euryarchaeota

Lei Cheng (✉ chenglei@caas.cn)
Key Laboratory of Development and Application of Rural Renewable Energy of Ministry of Agriculture
https://orcid.org/0000-0003-1178-8190

Kejia Wu
Biogas Institute of Ministry of Agriculture and Rural Affairs

Lei Zhou
Biogas Institute of Ministry of Agriculture and Rural Affairs

Guillaume Tahon
Wageningen University & Research https://orcid.org/0000-0001-7020-4162

Laiyan Liu
Biogas Institute of Ministry of Agriculture and Rural Affairs

Jiang Li
Biogas Institute of Ministry of Agriculture and Rural Affairs

Jianchao Zhang
Tianjin University

Fengfeng Zheng
Southern University of Science and Technology https://orcid.org/0000-0002-8507-162X

Chengpeng Deng
Biogas Institute of Ministry of Agriculture and Rural Affairs

Wenhao Han
Biogas Institute of Ministry of Agriculture and Rural Affairs

Li-ping Bai
Biogas Institute of Ministry of Agriculture and Rural Affairs

Lin Fu
Biogas Institute of Ministry of Agriculture and Rural Affairs

Xiuzhu Dong
Institute of Microbiology,Chinese Academy of Sciences https://orcid.org/0000-0002-6926-5459

Chuanlun Zhang
Southern University of Science and Technology (SUSTech)

Thijs Ettema
Wageningen University & Research https://orcid.org/0000-0002-6898-6377

Sousa Diana
Wageningen University & Research https://orcid.org/0000-0003-3569-1545

Biological Sciences - Article

Keywords:

Posted Date: February 14th, 2023

DOI: https://doi.org/10.21203/rs.3.rs-2501667/v1

Abstract

Methanogenic archaea are main contributors to methane emissions, and thus play a crucial role in carbon cycling and global warming. Until recently, methanogens were confined to the phylum Euryarchaeota, but metagenomic studies revealed the presence of genes encoding the methyl coenzyme M reductase complex in other archaeal clades, thereby opening up the premise that methanogenesis is taxonomically more widespread. Nevertheless, laboratory cultivation of these non-Euryarchaeal methanogens was missing to allow the study of their physiology and to corroborate their potential methanogenic capability. Here we describe a thermophilic co-culture from an oil field, containing a single archaeon (strain LWZ-6) belonging to the proposed order Candidatus Verstraetearchaeia, together with a H2-producing Acetomicrobium sp. CY-2. Strain LWZ-6, for which we propose the name Verstraetearchaeum methanopetracarbonis, is a H2-dependent methylotrophic methanogen. Although previous metagenomic studies speculated on the fermentative potential of Verstraetearchaeial methanogens, strain LWZ-6 does not ferment sugars, peptides, and amino acids. Its energy metabolism is linked to methanogenesis, with methanol and monomethylamine as electron acceptors and H2 as electron donor. Comparative (meta)genome analysis revealed that H2-dependent methylotrophic methanogenesis is a shared trait among Verstraetearchaeia. Our findings corroborate that the diversity of methanogens expands beyond the classical Euryarchaeota and change our current conception of the global carbon cycle.

Main Text

Methanogenic archaea represent one of the oldest life forms on Earth [1]. They are major contributors to global methane emissions, playing a significant role in climate change [2,3]. Based on the traditional 16S rRNA gene taxonomy, all the so far cultured methanogens are restricted to the archaeal phylum Euryarchaeota. Yet, the emergence of technologies allowing for deep sequencing of metagenomes from uncultured microbial communities challenged this view. In 2015, the key genes encoding the methyl-coenzyme M reductase (MCR) complex, a hallmark enzyme in methanogens [4], was discovered in two metagenome-assembled genomes (MAGs) of *Candidatus* (*Ca.*) Bathyarchaeota, suggesting the methanogenic potential in this non-Euryarchaeotal lineage [5]. Subsequently, the MCR complex genes and methanogenic pathway genes were identified in several uncultured non-Euryarchaeotal phyla, including *Ca.* Korarchaeota [6], *Ca.* Nezhaarchaeota [7], and *Ca.* Verstraetearchaeota [8-11]. Although introduced as a phylum, Verstraetearchaeota was later proposed to be a class within Thermoproteota (*Ca.* Verstraetearchaeia = *Ca.* Methanomethylicia), whereas *Ca.* Nezhaarchaeota was reclassified as an order (*Ca.* Nezhaarchaeales) within *Ca.* Verstraetearchaeia [12]. More recently, *Ca.* Culexarchaeia (now *Ca.* Culexarchaeales = B29_G17), a non-methanogenic lineage, further expanded *Ca.* Verstraetearchaeia [13]. However, the presence of MCR complex in MAGs is not sufficient proof of their methanogenic metabolism. For example, although members of *Ca.* Bathyarchaeia were first suggested to be potential methanogens, more recent studies indicate their MCR complex is more likely involved in short-chain hydrocarbon oxidation rather than in methanogenesis [14,15].

Methanogenesis is regarded as one of the most ancient biochemical pathways [1], and it is the only known energy conservation mechanism in methanogens [16]. Until now, five methanogenesis pathways have been characterized based on the type of substrate metabolized, *i.e.,* acetoclastic, alkylotrophic, hydrogenotrophic, methoxydotrophic, and methylotrophic methanogenesis [17-19]. Fermentative metabolism has been speculated for (potential) methanogens from the *Ca*. Bathyarchaeia [5] and *Ca*. Verstraetearchaeia [8] based on genomic analyses. Furthermore, MCR-containing MAGs from *Ca*. Korarchaeota encode the genes required for dissimilatory sulfur metabolism [6]. However, no cultivated representatives of methanogens from these new lineages have thus far been obtained, and therefore their physiology remains unclear.

Ca. Verstraetearchaeia has been predicted to possess both the potentials of methanogenesis and fermentation metabolism, such as glycolysis, peptide, and amino acids degradation [8,11,20]. These members are widely distributed, primarily in sediments of various anoxic environments, including hot springs, hydrothermal systems, marine and freshwater bodies, wetlands, and in oil and gas fields [21-23]. By applying a hybrid cultivation approach comprising of classical and high-throughput approaches throughout a 6-year period, we successfully obtained a stable co-culture containing only one *Ca*. Verstraetearchaeial and one bacterial species, enabling us to further investigate the physiology of methanogens beyond those affiliating with Euryarchaeota.

Establishment of a Verstraetearchaeial co-culture

Microorganisms affiliated with the *Ca.* Verstraetearchaeia were found to be rather rare in the original samples of oily sludge and oil-produced water in the Shengli oilfield (China), with a relative abundance of less than 1% of total archaea, as identified by 16S rRNA gene amplicon sequencing (Fig. 1a). After anaerobic incubation at temperatures ranging from 25 to 75 °C in basal medium with substrates such as acetate, propionate, butyrate, alkanes, or crude oil, *Ca*. Verstraetearchaeia members reached relative abundances of 8.1% - 82.5% at 45-65 °C (Extended Data Fig. 1). Subsequently, cultures showing high abundance of *Ca*. Verstraetearchaeia were 10-fold serially diluted in 96-well microplates with mixed substrates and incubated at 55 °C. After several transfers over consecutive years, the archaeal diversity was reduced to only one Verstraetearchaeon and one hydrogenotrophic methanogen, *Methanoculleus receptaculi* [24] (stage 3 in Fig. 1a). The simplified culture was then transferred into Hungate tubes supplemented with methanol without H_2/CO_2, and *M. receptaculi* was eventually eliminated upon subculturing for 3-4 times (Extended Data Fig. 2). At this point, the retained single archaeon culture was still accompanied by several bacterial taxa, which were again serially diluted and supplemented with antibiotics and lysozyme (see methods for details). Finally, a co-culture containing one Verstraetearchaeon (strain LWZ-6) and *Acetomicrobium* sp. CY-2 was obtained (stage 4 in Figs. 1a-b) and maintained these two strains after consecutive transfers (Extended Data Fig. 3). Based on the pairwise 16S rRNA gene identity and genomic average nucleotide identity (ANI) analysis, strain LWZ-6 is 100% and 97.2% related to *Ca.* Methanosuratincola petrocarbonis V4 (MAGV00000000) [8,25] (Fig. S2), respectively.

We here propose the Verstraetearchaeon as *Verstraetearchaeum methanopetracarbonis* strain LWZ-6(for taxonomic description, see Supplementary Note).

Catalyzed reporter deposition fluorescence in situ hybridization (CARD-FISH) and scanning electron microscopy (SEM) revealed that LWZ-6 cells were small (approximately 0.5 mm in diameter) and cocci-shaped, and that *Acetomicrobium* sp. CY-2 cells were rod-shaped (Figs. 1c-e, Extended Data Figs. 4a-f). These two microorganisms did not seem to aggregate during growth observed under light microscope (data not shown). No archaella was observed under transmission electron microscope (TEM) (Fig. 1f, Extended Data Fig. 4g-h). LWZ-6 lacked cofactor F_{420} autofluorescence with the blue-green light under the UV microscope, which is consistent with the absence of F_{420} biosynthesis genes in its genome (see below; Supplementary Table 4).

Strain LWZ-6 employs obligate hydrogen-dependent methylotrophic methanogenesis

To study the potential methanogenetic capacity of strain LWZ-6, we incubated the co-culture of strains LWZ-6 and CY-2 in fresh medium supplemented with methanol and added hydrogen to bottles' headspace. After 22 days of incubation at 55 °C, 0.44 ± 0.02 mmol methanol was used by the culture and methane accumulated up to 0.41 ± 0.02 mmol (Fig. 2a, Extended Data Figs. 5a-b). At this point, strain LWZ-6 reached 10^9 copies mL^{-1} as determined by quantitative PCR of the *mcrA* gene (Fig. 2a). The methanogenesis rate can be calculated as about 150 fmol $cell^{-1}$ day^{-1}. Both methane production and growth of strain LWZ-6 were inhibited by the addition of the common methanogenic inhibitor of 2-bromoethanesulfonate (BES) (Fig. 2b). Accumulation of hydrogen in tests with BES was most probably generated from the fermentation of yeast extract by the coexisting bacterium *Acetomicrobium* sp. CY-2 (Extended Data Figs. 5c, e, Fig. S3d). A H_2 consumption of 0.50 ± 0.09 mmol by the archaeon could be roughly calculated by subtracting the amount of hydrogen present in the setup to which BES was added from that without added BES (Fig. 2b). Taken together, a stoichiometry of one molar methanol and hydrogen converted to one molar methane could be calculated, in accordance with the reaction:

$$CH_3OH + H_2 \rightarrow CH_4 + H_2O.$$

To further verify methyl-reducing methanogenesis by strain LWZ-6, stable isotope tracing experiments supplemented with different ratios of ^{13}C-labeled methanol were performed. The heavy-carbon fraction in methane linearly increased with increasing initial ^{13}C-methanol supplementation, with a slope of 0.99 (Fig. 2c). While the generated $^{13}C/^{12}C$ ratio of CO_2 had a slight change from 1.08% to 1.44% (Extended Data Fig. 6), indicating that methanol is almost fully converted into methane. No labeled methane was produced when the co-culture was incubated with ^{13}C-labeled acetate or ^{13}C-labeled CO_2 (data not shown). Moreover, nanoscale secondary ion mass spectrometry (NanoSIMS) scanning and lipid stable isotope probing (lipid-SIP) analysis revealed no labeled methanol flows into biomass or lipid of strain LWZ-6 (Figs. 2d-g). Strain LWZ-6 also produces methane when grown on monomethylamine, but not on other C1-methylated compounds of dimethylamine, trimethylamine, and methanethiol (Extended Data Fig. 7a). Thus, these results confirmed that strain LWZ-6 employs hydrogen-dependent methylotrophic

methanogenesis as its energy conservation pathway. Lipid-SIP detected ^{13}C-labeled archaeol and methylated glycerol monoalkyl glycerol tetraether (Me-GMGT) fraction when strain LWZ-6 was incubated with ^{13}C-labeled acetate, CO_2, or yeast extract, indicating they are required as carbon sources (Fig. 2g).

In the co-culture, yeast extract or casamino acids, minimum at 0.05 g L^{-1}, were essential for growth of strain LWZ-6 (Extended Data Fig. 7b). The methanogenesis conditions of strain LWZ-6 was observed with optimum at 55 °C, pH 6.0-6.5 and 9-30 g L^{-1} NaCl, respectively (Extended Data Figs. 7c-e).

Reconstruction of the metabolic pathways of strain LWZ-6

The complete 1.54 megabase pair (Mbp) circular genome of strain LWZ-6 (DNA G+C content of 54.42%; 1606 open reading frames) was obtained by reassembly of Nanopore and Illumina sequencing data (Fig. S1, Supplementary Table 3). The genome contains the whole suite of genes encoding methanol methyltransferase (MtaABC) and for methanol reduction and methane production (McrABG) (Fig. 3, Supplementary Table 1). The genome harbors two copies of the monomethylamine transferase subunit (*mtmB*) but not the methylcobamide: CoM methyltransferase gene (*mtbA*) [29], which is most likely replaced by *mtaA* for monomethylamine reduction (Fig. 3, Supplementary Table 1). The genome lacks the archaeal methyl branch of Wood–Ljungdahl pathway (MBWL) genes involved in CO_2 reductive methanogenesis or methanol oxidative shunt in canonical methylotrophic methanogenesis, and N^5-methyltetrahydromethanopterin: coenzyme M methyltransferase (Mtr) complex (Fig. 3, Supplementary Tables 1, 2). This provides the genetic basis for strain LWZ-6 to perform obligate hydrogen-dependent methylotrophic methanogenesis.

Strain LWZ-6 may employ two mechanisms for heterodisulfide reduction. Genes encoding heterodisulfide reductase (HdrD) and cytoplasmic flavin adenine dinucleotide-containing dehydrogenase (GlcD) coupling an F_{420}-methanophenazine oxidoreductase like complex (Fpo-like) were detected. An energy-converting complex (Ehd) formed by a NiFe hydrogenase and HdrBC was identified in the LWZ-6 genome, suggesting that it may implement heterodisulfide reduction [10]. A proton gradient is generated by an energy-converting hydrogenase B complex (Ehb), Ehd, and Fpo-like complex drives V/A type ATP synthase to produce ATP (Fig. 3, Supplementary Tables 1 and 2). Absence of the MBWL pathways in the LWZ-6 genome leaves all the intermediate reactions in the methanogenic pathway unconnected with gluconeogenesis. We speculate that acetate conversion to acetyl-CoA, which is then combined with CO_2 to form pyruvate could be the pathway channeled to gluconeogenesis for biomass generation in strain LWZ-6 (Fig. 3).

The exponential phase culture of strain LWZ-6 grown on methanol and hydrogen was subjected to transcriptomic analysis. Genes of *mcrABG*, *mtaABC*, *hdrD,* and *glcD* ranked in the top 1% among the transcribed ones (Fig. 3, Supplementary Table 2), verifying the hydrogen-dependent methylotrophic methanogenesis activity of strain LWZ-6.

Expanded diversity of Verstraetearchaeia

We managed to obtain 23 Verstraetearchaeial MAGs from our various enrichment cultures. One MAG could be assigned to strain LWZ-6 and was replaced by the latter's complete genome sequence for the analyses. Genome completeness of the obtained MAGs ranged from 75 to 100% (Supplementary Table 3). Based on phylogenomic analysis and gene- and genome-level identities including publicly available MAGs from Verstraetearchaeia, the 23 genomes could be assigned to 3 genera and 5 species in the order Verstraetearchaeales. Of these, one MAG (Cluster 4) formed the first representative of a new genus. Two other MAGs (Cluster 2) formed a new species within an existing genus (Fig. 4, Fig. S2, Supplementary Table 3; See Supplementary Note for taxonomic descriptions). Analyses of 5 representative genomes – one from each of the 5 species-level clusters – indicated they all harbor the MCR complex and key genes for hydrogen-dependent methylotrophic methanogenesis (Fig. 4c, Supplementary Table 4). Phylogenomic tree reconstruction supplemented with 16S rRNA gene sequence similarity [30] and average amino acid identity (AAI) [31] using high-quality reference genomes covering the entire Verstraetearchaeia class confirmed the existence of three order-level clades: Verstraetearchaeales, *Ca*. Nezhaarchaeales and *Ca*. Culexarchaeales (Fig. 4a). Additionally, two MAGs could be assigned to a newly proposed order which we tentatively name *Ca*. Aukarchaeales, named after Auka hydrothermal vent from which one of the MAGs was recovered [32]. Genome mining revealed that all Verstraetearchaeales MAGs contained hydrogen-dependent methylotrophic methanogenesis pathways (Fig. 4c, Supplementary Table 4). The MAGs of *Ca*. Nezhaarchaeales and *Ca*. Culexarchaeales often lacked several of these key genes, although this could be due to genome incompleteness. Recovery of complete genomes from these lineages will reveal whether this pathway is also universally present in these orders. Interestingly, none of the *Ca*. Culexarchaeales MAGs had the potential for hydrogen-dependent methylotrophic methanogenesis, indicating that this capacity was lost when the Culexarchaeales lineages split from the common ancestor of Culexarchaeales and Nezhaarchaeales. Phylogenetic analysis of McrA and McrA-like homologs showed a highly supported Verstraetearchaeia clade in which distinct subclades of Verstraetearchaeales, *Ca*. Nezhaarchaeales and *Ca*. Aukarchaeales McrA could be observed (Fig. 4b), indicating that hydrogen-dependent methylotrophic methanogenesis is probably a widespread or even omnipresent physiological property for these lineages. Interestingly, we identified an McrA-like homolog in cluster 2 and cluster 4 Verstraetearchaeales MAGs that clustered with McrA sequences that have been shown to be involved in alkane oxidation. This indicates that, compared to strain LWZ-6, which belongs to cluster 1 in Verstraetearchaeles, clusters 2 and 4 have an expanded metabolic repertoire that includes the capacity to perform the oxidation of alkanes. However, this needs further cultivation verification.

Screening the Verstraetearchaeales-specific 16S rRNA genes and genomes indicated they are present in a variety of environments, particularly in subsurface sediments [8,11,20,22] (Extended Data Fig. 8, Supplementary Table 5). The environmental advantages of hydrogen-dependent methylotrophic methanogenesis over that of hydrogenotrophic methanogenesis can lie in the lower hydrogen partial pressures [33]. In addition, methylated compounds such as plant-derived methanol are abundant in nature [34,35]. Along with the confirmation of hydrogen-dependent methylotrophic methanogenesis and global distribution in subsurface environments of Verstraetearchaeia, several other methanogenic lineages

within the Euryarchaeota also implement hydrogen-dependent methylotrophic methanogenesis [35-38], highlighting the significance of such methanogenic pathway in global methane emissions.

Strain LWZ-6 is unable to perform fermentation growth

Investigation of the fermentation potential of strain LWZ-6 showed no active growth when it was incubated with glucose, pyruvate, or acetate without BES, and amino acids, casamino acids, keratin hydrolysates, or yeast extract with BES in the absence of methane production (Extended Data Table 1). Furthermore, we could neither identify genes encoding sugar transporter genes in the LWZ-6 genome, nor genes encoding pyruvate kinase (PYK) and phosphofructokinase (PFK) specific for the glycolysis pathway, while genes encoding phosphoenolpyruvate synthase (PPS) and fructose-1,6-bisphosphatase (FBP), both specific in the gluconeogenesis pathway, [36] could be found. The genes of peptide and amino acids transporters, aminotransferases and 2-oxoacid: ferredoxin oxidoreductases (Kor and Ior) and aldehyde ferredoxin oxidoreductases (Aor) could be involved in the biosynthesis of amino acids [37] (Fig. 3). Energy generation via fermentation was previously proposed via substrate-level phosphorylation by archaeal adenosine (ADP)-forming acetyl-CoA synthetase (Acd) converting acetyl-CoA to acetate [8]. AcdA and AcdB (alpha and beta subunits of Acd, respectively) display 52.95% and 50.88% amino acid sequence similarity to the AcdA and AcdB of the hyperthermophilic euryarchaeaon *Pyrococcus furiosus* DSM 3638^T, respectively. The *P. furiosus* Acd has been shown to exhibit an acetyl-CoA to acetate converting activity at 90 °C [38], whereas strain LWZ-6 grew optimally at 55 °C, a temperature at which Acd catalyzes the reverse reaction, converting acetate to acetyl-CoA [38,39]. Hence, this might explain why strain LWZ-6 was unable to carry out fermentative growth.

Conclusion

The field of archaeal methanogenesis has expanded significantly over the past decade, having witnessed the metagenomic discovery of a plethora of new lineages with the genetic potential for methane-related metabolisms, many of which unrelated to the ‘classical’ euryarchaeotal methanogens. Comparative genomic and phylogenetic analyses of these lineages have revealed a wide distribution of a wide variety of methanogenesis types across the archaeal tree of life indicating that methanogenesis and methane-associated pathways are ancient and that their origins potentially date back as far as to the last archaeal common ancestor [40]. The latter would imply that the current diversity of archaea is the result of a complex evolutionary trajectory that includes pervasive loss and tinkering of genes involved in methane metabolism [19]. While the metagenomic exploration of new methanogenic lineages has provided exciting new insights into the evolution of methanogenesis, the vast majority of these lineages remain, however, uncultured.

Being based uniquely on sequence analysis, our knowledge of the metabolic potential of these new players in global methane cycling remains limited, lacking detailed information about their physiology and ecology. Here we have isolated and characterized the first methanogen outside Euryarchaeota,

Verstraetearchaeum methanopetracarbonis LWZ-6, and demonstrated that it employs hydrogen-dependent methylotrophic methanogenesis as the exclusive energy conservation path, rather than alternative metabolism predicted from metagenomics analysis. Additionally, LWZ-6 produces methane at a parallel rate and yield as the Euryarchaeotal ones [41], further indicating that it represents an authentic methanogen. Recent metagenomic studies have revealed that potential hydrogen-dependent methylotrophic methanogens, including those that are part of the Verstraetearchaeia, are globally distributed across various anaerobic subsurface environments [23]. Hence, considering the role of methane as an especially potent greenhouse gas, the significance of hydrogen-dependent methylotrophic methanogenesis in methane-emitting environments deserves reevaluation as it is likely to impact efforts to model the global methane emissions.

Declarations

Acknowledgements

We thank P. Geesink (Wageningen University & Research) for performing Nanopore sequencing of strain LWZ-6. W. B. Whitman (University of Georgia) for comments on the manuscript; L.-r. Dai, M. Yang, and L. Fu for assisting in cultivation and experiments; and Z. Zhou for technical support. This study was supported by National Natural Science Foundation of China (92051108, 31970066, 42203080, and 42207167), Agricultural Science and Technology Innovation Project of the Chinese Academy of Agriculture Science (CAAS-ASTIP2016-BIOMA), Netherlands Ministry of Education, Culture and Science (Project 024.002.002: Soehngen Institute of Anaerobic Microbiology), European Research Council (grant 817834), and the Dutch Research Council (grant VI.C.192.016)

Authors contributions

L.C. initiated the study. L.C., D.S., K.-J.W., T.J.G.E., and L.Z. designed the research. L.-Y.L. performed the initial cultivation. K.-J.W., L.Z., L.-Y.L., and J.L. carried out the isolation process and physiological experiments. G.T. and W.-H.H. performed all bioinformatics analyses. C.-P.D. performed CARD-FISH, J.-C.Z. performed NanoSIMS, F.-F.Z. and C.-L.Z. performed lipid-SIP. L.F. and L.-P.B. performed biochemical analysis. K.-J.W. and L.Z. analyzed data. X.-Z.D. provided constructive suggestion on the isolation process. K.-J.W., L.C., X.-Z.D., T.J.G.E., and D.S. wrote the manuscript with the contributions from all the co-authors.

Competing interests

The authors declare no competing interest.

Data availability

The 16S rRNA gene amplicon sequences, metagenomic, genomic, and transcriptome data generated in the current study are available in the NODE database

(https://www.biosino.org/node/project/detail/OEP003742). Further details are listed in Supplementary Table 7. All other data are presented in the main text or the Supplementary Information.

Code availability

The codes and programs used for analyses are mentioned in the Methods, they are also available at GitHub https://github.com/zhuozhou1993/Methanosuratus/blob/main/code.

References

1. Thauer, R. K., Kaster, A.-K., Seedorf, H., Buckel, W. & Hedderich, R. Methanogenic archaea: ecologically relevant differences in energy conservation. *Nat. Rev. Microbiol.* **6**, 579-591 (2008).
2. Saunois, M. et al. The global methane budget 2000–2017. *Earth system science data* **12**, 1561-1623 (2020).
3. Ferry, J. G. *Methanogenesis: ecology, physiology, biochemistry & genetics*. (Springer Science & Business Media, 2012).
4. Ermler, U., Grabarse, W., Shima, S., Goubeaud, M. & Thauer, R. K. Crystal structure of methyl-coenzyme M reductase: the key enzyme of biological methane formation. *Science* **278**, 1457-1462 (1997).
5. Evans, P. N. et al. Methane metabolism in the archaeal phylum Bathyarchaeota revealed by genome-centric metagenomics. *Science* **350**, 434-438 (2015).
6. McKay, L. J. et al. Co-occurring genomic capacity for anaerobic methane and dissimilatory sulfur metabolisms discovered in the Korarchaeota. *Nat. Microbiol.* **4**, 614-622 (2019).
7. Wang, Y., Wegener, G., Hou, J., Wang, F. & Xiao, X. Expanding anaerobic alkane metabolism in the domain of Archaea. *Nat. Microbiol.* **4**, 595-602 (2019).
8. Vanwonterghem, I. et al. Methylotrophic methanogenesis discovered in the archaeal phylum Verstraetearchaeota. *Nat. Microbiol.* **1**, 16170 (2016).
9. Berghuis, B. A. et al. Hydrogenotrophic methanogenesis in archaeal phylum Verstraetearchaeota reveals the shared ancestry of all methanogens. *P. Natl Acad. Sci. USA* **116**, 5037-5044 (2019).
10. Borrel, G. et al. Wide diversity of methane and short-chain alkane metabolisms in uncultured archaea. *Nat. Microbiol.* **4**, 603-613 (2019).
11. Kadnikov, V. et al. Genome of a member of the candidate archaeal phylum Verstraetearchaeota from a subsurface thermal aquifer revealed pathways of methyl-reducing methanogenesis and fermentative metabolism. *Microbiology* **88**, 316-323 (2019).
12. Parks, D. H. et al. GTDB: an ongoing census of bacterial and archaeal diversity through a phylogenetically consistent, rank normalized and complete genome-based taxonomy. *Nucleic Acids Res.* **50**, D785-D794 (2022).
13. Kohtz, A. J., Jay, Z. J., Lynes, M. M., Krukenberg, V. & Hatzenpichler, R. Culexarchaeia, a novel archaeal class of anaerobic generalists inhabiting geothermal environments. *ISME Commu.* **2**, 86

(2022).

14. Laso-Pérez, R. et al. Thermophilic archaea activate butane via alkyl-coenzyme M formation. *Nature* **539**, 396-401 (2016).
15. Wang, Y., Wegener, G., Ruff, S. E. & Wang, F. Methyl/alkyl-coenzyme M reductase-based anaerobic alkane oxidation in archaea. *Environ. Microbiol.* **23**, 530-541 (2021).
16. Mand, T. D. & Metcalf, W. W. Energy conservation and hydrogenase function in methanogenic archaea, in particular the genus *Methanosarcina*. *Microbiol. Mol. Biol. Rev.* **83**, e00020-00019 (2019).
17. Zhou, Z. et al. Non-syntrophic methanogenic hydrocarbon degradation by an archaeal species. *Nature* **601**, 257-262 (2022).
18. Mayumi, D. et al. Methane production from coal by a single methanogen. *Science* **354**, 222-225 (2016).
19. Garcia, P. S., Gribaldo, S. & Borrel, G. Diversity and evolution of methane-related pathways in archaea. *Annu. Rev. Microbiol.* **76**, 727-755 (2022).
20. Liu, Y.-F. et al. Long-term cultivation and meta-omics reveal methylotrophic methanogenesis in hydrocarbon-impacted habitats. *Engineering* (2022).
21. Liu, Y.-F. et al. Anaerobic degradation of paraffins by thermophilic Actinobacteria under methanogenic conditions. *Environ. Sci. Technol.* **54**, 10610-10620 (2020).
22. Hua, Z.-S. et al. Insights into the ecological roles and evolution of methyl-coenzyme M reductase-containing hot spring Archaea. *Nat. Commun.* **10**, 1-11 (2019).
23. Evans, P. N. et al. An evolving view of methane metabolism in the Archaea. *Nat. Rev. Microbiol.* **17**, 219-232 (2019).
24. Cheng, L. et al. Isolation and characterization of *Methanoculleus receptaculi* sp. nov. from Shengli oil field, China. *FEMS. Microbiol. Lett.* **285**, 65-71 (2008).
25. Oren, A., Garrity, G. M., Parker, C. T., Chuvochina, M. & Trujillo, M. E. Lists of names of prokaryotic Candidatus taxa. *Int. J. Syst. Evol. Microbiol.* **70**, 3956-4042 (2020).
26. Stahl, D. A. Development and application of nucleic acid probes. *Nucleic acid techniques in bacterial systematics*, 205-248 (1991).
27. Klindworth, A. et al. Evaluation of general 16S ribosomal RNA gene PCR primers for classical and next-generation sequencing-based diversity studies. *Nucleic Acids Res.* **41**, e1-e1 (2012).
28. Daims, H., Brühl, A., Amann, R., Schleifer, K.-H. & Wagner, M. The domain-specific probe EUB338 is insufficient for the detection of all Bacteria: development and evaluation of a more comprehensive probe set. *Syst. Appl. Microbiol.* **22**, 434-444 (1999).
29. Lang, K. et al. New mode of energy metabolism in the seventh order of methanogens as revealed by comparative genome analysis of *Candidatus* Methanoplasma termitum. *Appl. Environ. Microbiol.* **81**, 1338-1352 (2015).
30. Yarza, P. et al. Uniting the classification of cultured and uncultured bacteria and archaea using 16S rRNA gene sequences. *Nat. Rev. Microbiol.* **12**, 635-645 (2014).

31. Konstantinidis, K. T., Rosselló-Móra, R. & Amann, R. Uncultivated microbes in need of their own taxonomy. *ISME J.* **11**, 2399-2406 (2017).
32. Speth, D. R. et al. Microbial community of recently discovered Auka vent field sheds light on vent biogeography and evolutionary history of thermophily. Preprint bioRvix: https://doi.org/10.1101/2021.1108.1102.454472 (2021).
33. Feldewert, C., Lang, K. & Brune, A. The hydrogen threshold of obligately methyl-reducing methanogens. *FEMS. Microbiol. Lett.* **367**, fnaa137 (2020).
34. Zhuang, G.-C., Lin, Y.-S., Elvert, M., Heuer, V. B. & Hinrichs, K.-U. Gas chromatographic analysis of methanol and ethanol in marine sediment pore waters: Validation and implementation of three pretreatment techniques. *Mar. Chem.* **160**, 82-90 (2014).
35. Zhuang, G.-C., Peña-Montenegro, T. D., Montgomery, A., Hunter, K. S. & Joye, S. B. Microbial metabolism of methanol and methylamine in the Gulf of Mexico: insight into marine carbon and nitrogen cycling. *Environ. Microbiol.* **20**, 4543-4554 (2018).
36. Verhees, C. H. et al. The unique features of glycolytic pathways in Archaea. *Biochem. J.* **375**, 231-246 (2003).
37. Tersteegen, A., Linder, D., Thauer, R. K. & Hedderich, R. Structures and functions of four anabolic 2-oxoacid oxidoreductases in *Methanobacterium thermoautotrophicum*. *Eur. J. Biochem.* **244**, 862-868 (1997).
38. Glasemacher, J., Bock, A. K., Schmid, R. & Schönheit, P. Purification and properties of acetyl-CoA synthetase (ADP-forming), an archaeal enzyme of acetate formation and ATP synthesis, from the hyperthermophile *Pyrococcus furiosus*. *Eur. J. Biochem.* **244**, 561-567 (1997).
39. Musfeldt, M. & Schönheit, P. Novel type of ADP-forming acetyl coenzyme A synthetase in hyperthermophilic archaea: heterologous expression and characterization of isoenzymes from the sulfate reducer *Archaeoglobus fulgidus* and the methanogen *Methanococcus jannaschii*. *J. Bacteriol.* **184**, 636-644 (2002).
40. Adam, P. S., Kolyfetis, G. E., Bornemann, T. L., Vorgias, C. E. & Probst, A. J. Genomic remnants of ancestral methanogenesis and hydrogenotrophy in Archaea drive anaerobic carbon cycling. *Sci. Adv.* **8**, eabm9651 (2022).
41. Beulig, F., Røy, H., McGlynn, S. E. & Jørgensen, B. B. Cryptic CH_4 cycling in the sulfate–methane transition of marine sediments apparently mediated by ANME-1 archaea. *ISME J.***13**, 250-262 (2019).

Methods

Data reporting.

No statistical methods were used to predetermine sample size. The experiments were not randomized, and investigators were not blinded to allocation during experiments and outcome assessment.

Enrichment and cultivation conditions

The oily sludge and oil-produced water used as inoculum were collected from the Shengli oilfield in China (37°54'N, 118°33'E). Upon collection, samples were stored anaerobically at 4 °C. Additional details and parameters of the oily sludge were described previously [17]. The basal medium for incubation was made of 9 g L^{-1} NaCl, 0.3 g L^{-1} $MgCl_2 \cdot 6H_2O$, 0.15 g L^{-1} $CaCl_2 \cdot 2H_2O$, 0.3 g L^{-1} NH_4Cl, 0.2 g L^{-1} KH_2PO_4, 0.5 g L^{-1} KCl, 0.5 g L^{-1} cysteine-HCl, 1 mL L^{-1} resazurin solution and 2 mL L^{-1} trace element solution [42]. The medium was boiled for 30 min and then dispensed in serum bottles (Shuniu) with butyl rubber stoppers (Bellco Glass). The headspace was replaced by 99.999% oxygen-free N_2. After sterilization at 121°C for 30 min, the basal medium was supplied with filter-sterilized vitamin mixture (2 mL L^{-1}) [43], vitamin B_{12} (2 mL L^{-1}) and vitamin B_1 (2 mL L^{-1}) solutions. Fresh medium was made of the basal medium supplied with 10 mg L^{-1} filter-sterilized 2-mercaptoethanesulfonic acid (CoM), 1% selenite-tungstate solution [44], 0.5 g L^{-1} yeast extract, and 20 mM 2-morpholinoethanesulfonic acid monohydrate (MES) buffer. 1 M HCl or NaOH solutions were used to adjust the pH of media to 6.5-7.0 prior to use. The oil-produced water incubated with autoclaved 20 mM acetate, 20 mM propionate, 20 mM butyrate, and oily sludge incubated with *n*-hexadecane (1 mL L^{-1}, Sigma-Aldrich), eicosane (1 mL L^{-1}, Sigma-Aldrich), alkanes mix including *n*-docosane (1 g L^{-1}, Sigma-Aldrich), *n*-hexadecylcyclohexane (1 mL L^{-1}, TCI), and *n*-hexadecylbenzene (1mL L^{-1}, TCI), or and crude oil (1 g L^{-1}) as substrates in basal medium were performed at temperatures from 25 °C to 75 °C. The enrichments with the relative abundance of Verstraetearchaeia above 20% were chosen for further isolation (Extended Data Fig. 1). These cultures were 10-fold serially diluted in 96-well microplates with fresh medium of different compositional substrates (10 mM acetate, 10 mM glucose, 10 mM methanol, 10 mM lactate, 10 mM pyruvate, 10 mM succinate, 10 mM formate, 0.5 g L^{-1} casamino acids, 0.5 g L^{-1} rumen fluid) at 55 °C. Detection of Verstraetearchaeia in 96-well microplates was determined by PCR with specific- Verstraetearchaeia primer (MSR4F/MSR4R, Supplementary Table 6). After 3 times transfer with dilution of 1:100000 in mixed substrates of acetate, methanol, and lactate, Verstraetearchaeia was detected. These positive Verstraetearchaeia cultures in 96-well microplates were transferred into 10 mL Hungate tubes. Consecutive subcultures with dilutions varying from 0.1%-10% in fresh medium supplemented with 10 mM methanol were then conducted in the Hungate tubes. To remove bacteria, 10-fold serial dilutions supplemented with 500 mg L^{-1} lysozyme and several antibiotics including 100 mg L^{-1} ampicillin, 10 mg L^{-1} chloramphenicol, 100 mg L^{-1} gentamicin, 100 mg L^{-1} kanamycin, 100 mg L^{-1} streptomycin, and 50 mg L^{-1} vancomycin separately or mixed together were used.

If not especially mentioned, the Verstraetearchaeial cultures were incubated in 120 mL serum bottles with 50 mL fresh medium, 10 mM methanol, and 10 kPa hydrogen at 55 °C. BES was added to a concentration of 10 mM. Methylated compound utilization was examined by adding 5 mM dimethylamine, 5 mM methanol, 5 mM methanethiol, 5 mM monomethylamine or 5 mM trimethylamine into fresh medium at 55 °C. Temperature, pH, salt tolerance, and essential growth factors tests were determined as previously described [45]. All incubations were performed triplicate in the dark without shaking.

In the stable isotope tracer experiment, 1, 2, 4, and 8 % ^{13}C-labeled methanol (Sigma, USA) was made by mixing 0.1 mL, 0.2 mL, 0.4 mL, and 0.8 mL 0.05 M ^{13}C-labeled with 0.495 mL, 0.49 mL, 0.48 mL, and 0.46 mL 1 M unlabelled methanol, respectively. 0.5 mL 1 M unlabelled methanol was used as the control group. Methanol was added to a final concentration of 10 mM. The actual content of the initial labelled methanol was measured by Delta V advantage (Thermo Fisher). To determine the utilization of carbon sources, 5 mM 1,2-^{13}C-acetate (Sigma, USA), 1% (w/w) ^{13}C-$NaHCO_3$ (Sigma, USA), or 0.5 g L^{-1} ^{13}C-yeast extract were carried out in fresh medium with 10 mM unlabeled methanol. 10 mM ^{13}C-methanol was performed in fresh medium. The ^{13}C-yeast extract was made from the labeled ^{13}C cell extract of *Pichia pastoris* [46]. Briefly, *P. pastoris* was incubated in a minimal medium [46] with 2 g L^{-1} $^{13}C_6$-D-glucose (Sigma, USA) as the sole carbon source. After incubation for 4 days at 28 °C, the cells were centrifuged at 8000 g for 10 min and washed with phosphate-buffered saline (PBS, 1 M, pH 6.8) three times. The washed cells were then ultrasonicated on ice for 50 min. The supernatant from the ultrasonic cells was collected and the precipitation was ultrasonicated in 50% methanol for 10 min twice and centrifuged. All the supernatant was freeze-dried for further use. All the incubations were performed in triplicate at 55 °C in the dark without shaking.

To determine the fermentation growth, the Verstraetearchaeial co-culture (strain LWZ-6/CY-2) was incubated with 20 mM acetate, 20 mM glucose, 20 mM pyruvate, or 5 g L^{-1} yeast extract in fresh medium, and 4 mM 20 amino acids mix with 10 mM BES in fresh medium (0.5 g L^{-1} yeast extract changed into 0.05 g L^{-1}), and 5 g L^{-1} casamino acids, 5 g L^{-1} keratin hydrolysates or 5 g L^{-1} yeast extract with 10 mM BES in fresh medium (without 0.5 g L^{-1} yeast extract). 20 amino acids include alanine, arginine, aspartate, cysteine, methionine, glutamate, glycine, histidine, lysine, L-Asparagine, L-glutamine, L-isoleucine, L-leucine, L-Phenylalanine, L-Proline, L-Serine, L-Threonine, L-Tryptophan, L-Tyrosine, L-Valine. All the incubations were performed in triplicate at 55 °C in the dark without shaking.

Methane production and qPCR were used to determine the growth of strain LWZ-6. The specific growth or methane production rate (μ) of strain LWZ-6 at the log phase was calculated according to the equitation (1): $\mu = \frac{lnX2 - lnX1}{t2 - t1}$ (1), which means the doubling copy numbers or methane production from X_1 to X2 at incubation time from t_1 to t_2. The methanogenetic rate was calculated according to the equitation previously described [47].

Chemical analysis

The concentration of CH_4 and CO_2 in the headspace was measured by using an Agilent GC 7820A gas chromatography (GC) system equipped with a Porapak Q column (length, 3 m; inner diameter, 0.32 mm) and a thermal conductivity detector (TCD) [48] using hydrogen (99.999%) as carrier gas at a flow rate of 27 mL min^{-1}. The GC temperature of injection, column, and TCD was 65 °C, 120 °C, and 130 °C, respectively. The concentration of H_2 in the headspace was determined using the same Agilent GC 7820A parameters with nitrogen as carrier gas at a flow rate of 38 mL min^{-1}. The gas pressure in Hungate tubes or serum

bottles was measured using a barometer (Ashcroft) at room temperature. Each measurement was carried out by injection of 0.1 mL gas using a pressure lock syringe (Vici) at room temperature.

Methanol was measured by using an Agilent GC 7890A gas chromatography system equipped with a DB-WAX column (length, 30 m; inner diameter, 0.32 mm) and a flame ionization detection (FID) using nitrogen (99.999%) as carrier gas at a flow rate of 27 mL min^{-1}. The initial oven temperature was 50 °C, held for 1 min, and increased to a temperature of 220 °C at the rate of 60 °C min^{-1}, FID temperature remained at 250 °C. Acetate was determined by high-performance liquid chromatography (Agilent HPLC 1200) [49].

The carbon isotopic compositions of CH_4 and CO_2 in the headspace were determined by coupling gas chromatography and a mass spectrometer (IsoPrime100) [50]. Briefly, CH_4 and CO_2 in gas samples were first divided by GC (Agilent GC 7890B) with an HP-PLOT/Q column (30 m; inner diameter, 0.32 mm; film thickness, 20 μm). The carrier gas is helium (99.999%) at a flow rate of 2.514 mL min^{-1}. The oven and injector temperatures were 60 °C and 105 °C, respectively. The CH_4 was then converted to CO_2 in a combustion furnace (IsoPrime) at a temperature of 1050 °C. The carbon isotopic composition of CO_2 was measured by the IsoPrime100 isotope ratio mass spectrometer. The carbon isotope composition of methanol was determined by Delta V advantage (Thermo Fisher) coupled with TraceGC 3000 and equipped with column HP-INNOWAX (30 m*0.25 mm*0.25 μm, USA) using helium (99.999%) as carrier gas at a flow rate of 1.5 mL min^{-1}. BCR-653 WINE (EtOH, low level) (JRC-IRMM) was used as standard.

The labeled methanol in the medium and labeled CH_4 in the headspace was calculated by equations (2) and (3), respectively.

$$\text{Labeled methanol (mol)} = \text{total methanol} * {}^{13}\text{C methanol content} - \text{total methanol} * {}^{13}\text{C methanol in control group} \quad (2)$$

$$\text{Labeled } CH_4 \text{ (mol)} = \text{total } CH_4 * {}^{13}\text{C } CH_4 \text{ content} - \text{total } CH_4 * {}^{13}\text{C } CH_4 \text{ content in control group} \quad (3)$$

DAPI staining

Cells were collected and centrifuged at 16000 g for 10 min. The cells were then washed by PBS (1 M, pH 6.8) twice and fixed in 4% formaldehyde for 3 h. The fixed cells were washed again and mixed with Mini-Q water. Cells were dropped on the slide and dyed with 2-(4-Amidinophenyl)-6-indolecarbamidine dihydrochloride (DAPI) staining solution (Beyotime Biotechnology). The dyed cells were dried and mounted with antifade mounting medium (Beyotime Biotechnology). The mounted slide was imaged under laser scanning confocal microscope observation (ZEISS).

CARD-FISH

Samples were fixed in 4 % formaldehyde for 3 h and then washed with PBS (1 M, pH 6.8). The cells were filtrated on a 0.22 μm filter. Embedding was carried out with 0.2% agar on the filter. The embedded filter was then dehydrated with 96% pure ethanol. Permeabilization of the samples was performed with lysozyme solution (0.05 M EDTA pH 8.0, 0.1 M Tris/HCl pH 8.0, 10 mg mL^{-1} lysozyme, Sigma-Aldrich) at 37 °C for 60 min and proteinase K solution (0.05 M EDTA pH 8.0, 0.1 M Tris/HCl pH 8.0, 15 μg mL^{-1} proteinase K, Merck) at room temperature for 5 min. Inactivation of cells was conducted by incubating with endogenous peroxidases (10 mL methanol, 50 mL 30% H_2O_2) at room temperature for 30 min. The samples were hybridized with 16S rRNA gene-specific oligonucleotide probes of EUB-338 targeting bacteria and ARCH-915 [26,51] for Archaea (Takara Bio). The optimal formamide concentration in hybridization buffer for the stringency of probes was tested with increasing formamide concentrations (20%-45%). 20% and 35% formamide were chosen for EUB-338 and ARCH-915 for hybridization, respectively. Double hybridization was carried out after inactivation of peroxidases from the first hybridization. The signal amplification was continued using tyramide in dark conditions. Alexa Fluor 488 and Alexa Fluor 594 (AAT Bioquest, Inc) were used for laser scanning confocal microscope observation (ZEISS).

SEM

Cells were fixed with 2.5% glutaraldehyde for 1 h at room temperature. Samples were then washed with sterilized ultra-pure water for 5 min twice. Dehydration of the samples using serial ethanol concentration (30%, 50%, 70%, 80%, 90%, 95%, and 100%, each for 10 min) was performed. Cells were finally sputter coated with osmium (Hitachi, Ltd) and observed under SEM (FEI Company).

TEM

Samples were fixed with 3% glutaraldehyde and then with 1% osmium tetroxide. The cells were dehydrated with acetone by a serial concentration of 30%, 50%, 70%, 80%, 90%, and 95% once and 100% three times. Then the cells were incubated in a mixture of acetone and resin (Quetol-812: Nissin) with a ratio of 3:1, 1:1, 1:3, and polymerized with resins. The polymerized cells were ultrathin sectioned at 60-90 nm by ultramicrotome (UC&rt, LEICA) and sections were mounted on copper grids. The grids were stained with uranyl acetate for 15 min and then stained with lead stain solution for 2 min, after which the grids were imaged by a transmission electron microscope (JEOL).

NanoSIMS

The cells were fixed in 2.5% glutaraldehyde for 2 h. The fixed samples were then rinsed three times in PBS buffer to remove excess glutaraldehyde. The rinsed samples were dropped onto silicon wafers, and then dehydrated sequentially with 25%, 50%, 80%, and 100% solutions of ethanol. SEM imaging was used to localize regions of interest (ROI) with cocci cells of LWZ-6 for further NanoSIMS analysis. Prior to SEM imaging, the wafers were coated with 5 nm platinum. SEM was conducted on a Zeiss EVO18 at a working distance of 6 mm and an electron high tension of 2.0 kV. The wafer samples were further

analyzed with NanoSIMS 50L (CAMECA) using a Cs^+ primary source [52,53]. Secondary ions of ^{12}C and ^{13}C were collected by electron multipliers. The samples were scanned in 10 × 10 μm^2 area with 256 × 256 pixel raster. The $^{13}C/^{12}C$ ratios of the ROI were measured with the OpenMIMS plugin in ImageJ. All images were corrected for the electron multiplier dead time (44 ns) as well as drift corrected.

Lipid-SIP

Lipids of the culture cell were extracted using an acid hydrolysis extraction method [54]. In brief, the culture cells were collected by centrifugation at 12000 g for 10 min, the cells were acid hydrolyzed by 10% hydrochloric acid in methanol and then phase separated by adding dichloromethane (DCM) and ultrapure water. The total lipid extracts (TLEs) were filtered and dried prior to analysis.

The TLEs were analyzed by a Waters ACQUITY *I*-Class Ultra-performance liquid chromatography (UPLC) coupled to an SYNAPT G2-S*i* quadrupole time-of-flight (qTOF) high-resolution mass spectrometer (HRMS) through an electrospray ionization (ESI). The MS setting was identical to that previously described [55]. The mass acquisition mode was Fast-DDA (digital differential analyzer) with a mass range for MS m/z 100–2000 and MS^2 m/z 50–2000.

The raw data were processed with Masslynx software (V4.1). The unlabeled samples were employed for lipid structure identification, according to exact molecular mass and MS^2 fragment spectra. The degree of ^{13}C stable isotope labeling into lipids was estimated based on their MS1 mass spectra following calculations by Thiele and Matsubara [56]. Two representative archaeal lipids [57], archaeol ($C_{43}H_{88}O_3$) and Me-GMGT ($C_{87}H_{160}O_6$) were selected for the calculation of labeling degree. The mass range of isotoplogs was narrowed to *m/z* 650-710 for archaeol and *m/z* 1300-1400 for Me-GMGT. The base peak intensity of an isotoplog with *i* ^{13}C atoms (BPI_i) was calculated by normalizing it to the highest intensity of all isotoplogs, which was further normalized to the sum BPI of all isotoplogs, resulting in the $BPI_{i(norm)}$. The degree of ^{13}C labeling of an isotopolog with *i* ^{13}C atoms (DoL_i) and the total degree of ^{13}C labeling of a lipid (DoL) was calculated with the following equations:

$$\mathrm{DoL}i = \frac{\mathrm{BPIi(norm)}*\mathrm{i}}{\mathrm{n}} \quad (4)$$

$$DoL = \sum_{i=0}^{n} \mathrm{DoL}i \quad (5)$$

i refers to the number of ^{13}C atoms; *n* refers to the number of ^{13}C in a molecule.

DNA and RNA extraction

DNA was extracted by bead-beating (Sigma, ≤106 μm) methods combined with an Ezup Column Bacteria Genomic DNA Purification Kit (Sangon Biotech) according to the manufacturer's protocol. DNA

concentration was measured using a NanoDrop 2000 spectrophotometer (Thermo Scientific), and DNA was stored at −80 °C until further processing.

RNA extraction was conducted using bead-beating for releasement and extracted by using an RNAprep Pure Cell /Bacteria Kit (TIANGEN Biotech Co, Ltd.) according to the manufacturer's protocol.

qPCR

Quantitative PCR (qPCR) was performed to quantify the bacteria, and *Methanoculleus* using the primers targeting their 16S rRNA gene of 519F/907R[58], and ZC2F/ZC2R (Supplementary Table 6), respectively, and primers targeting on 16S rRNA gene and *mcrA* gene for strain LWZ-6 of MSR4F/MSR4R and mcrA4F/mcrA4R (Supplementary Table 6). The qPCR primers of strain LWZ-6 and *Methanoculleus* were designed by using NCBI/Primer-BLAST [61]. The qPCR process was performed following the previous description [16]. The standard DNA for qPCR of bacteria, *Methanoculleus* and strain LWZ-6 were obtained from the 16S rRNA gene of *E.coli* DH5α and *Methanoculleus recpetaculi* ZC-2^T, and the 16S rRNA gene and *mcrA* gene of strain LWZ-6. The qPCR for each targeted gene was determined in triplicate. PCR and qPCR products were sequenced by Sanger sequencing (Sangon Biotech).

16S rRNA gene amplicon sequencing

1 mL culture was taken for DNA extraction to amplicon sequencing. 16S rRNA gene was amplified using the primers sets for bacteria with barcode (341F/806R) [27,59], primers set for archaea Arch519F/Arch915R (Supplementary Table 6) [60], and universal primers targeting both bacteria and archaea with barcode 515FmodF/806RmodR [61] (Supplementary Table 6). The amplicon product was then sequenced by a NovaSeq6000 sequencer (Illumina) with paired-end 250 bp mode (PE250) at Novogene Bioinformatics Technology (Novogene). All the sequence data were first filtered to remove the low-quality reads [62,63]. Further reads were analyzed according to the Qiime2 pipeline [64]. The sequences were clustered into operational taxonomic units (OTUs; 97% similarity). The taxonomy was determined by using the Naive Bayes method in Qiime2 and the Silva NR99 database (release138) as the reference [65,66].

Metagenome sequencing, assembly, genome binning, and annotation

Genomic DNA was extracted and sent to Novogene for library sequencing using a NovaSeq 6000 platform with PE150, generating raw metagenomic sequencing data. The raw reads were processed as follows: qualified trimmed reads were obtained using Trimmomatic v.0.38 [67]. De novo assembly was performed using metaSPAdes (v.3.12.0) with the *k*-mer sizes (21, 33, 55, 77) [68]. Genome binning of the assemblies was proceeded using BBMap (v.38.24) and MetaBAT (v.2.12.1). The ambiguous contigs and redundant contigs were removed from binning. Completeness, contamination, and strain heterogeneity were identified using CheckM to evaluate the estimated quality and completeness of each recovered MAGs [69]. Taxonomic classification of MAGs was performed according to the GTDB database (release95.0, July 2020) [70]. 2 A total of 23 MAGs grouping with Verstraetearchaeia (i.e. *Ca*.

Methanomethylicia) were retrieved from the enrichments. Similarity of each MAG with the other MAGs and publicly available Verstraetearchaeia MAGs was determined using the 16S rRNA gene sequence identity, the average amino acid identity (AAI), the average nucleotide identity (ANI), and the percentage of conserved proteins (POCP) with other published Verstraetearchaeia MAGs. Barrnap was used to obtain the 16S rRNA gene sequences (https://github.com/tseemann/barrnap). ANI of the MAGs was calculated by OrthoANIu (Orthologous ANI using USEARCH) tool [71]. The AAI was calculated with CompareM (V0.1.2) (https://github.com/dparks1134/CompareM). POCP calculation was followed by Qin et al [72]. The 23 MAGs could be dereplicated [73] into 5 species-level clusters by using an ANI cut-off of 97% (Supplementary Table 3). One MAG was chosen per cluster for downstream analyses. These MAGs were first analyzed by prodigal (v.2.6.3) [74], and then annotation of open reading frames (ORFs) was predicted by using the KEGG server (BlastKOALA) [75] and eggnog-mapper v2 [76]. The predicted genes ascribing to methanogenesis were further verified using Uniprot [77] and CD-search (conserved domain) in NCBI [78].

Nanopore for closed genome binning and analysis

Metagenome sequencing of the simple culture (stage 3 in Fig. 1) was conducted as described above. The Illumina metagenome was assembled using metaSPAdes v3.13.0 [68] under default parameters. Subsequent binning of the contigs using MetaWRAP v1.3 [79] gave a Verstraetearchaeial bin (1.54 Mb, 2 contigs). Nanopore data was generated to close the genome: the library was prepared with 60 ng genomic DNA using the ligation sequencing gDNA kit (ONT) following the manufacturer's instructions and minor modifications. In short, DNA repair and end-prep were performed using the NEBNext FFPE DNA Repair Mix and NEBNext Ultra II End repair/dA-tailing Module (New England Biolabs), followed by the adapter ligation using Quick T4 ligase (New England Biolabs). Subsequently, a clean-up using AMPure beads (Beckman Coulter) and the short fragment buffer (SFB) was performed to retain DNA fragments of all sizes with a final incubation at 37 °C for 10 min. The library was then directly loaded onto a primed SpotON R9.4.1 flow cell in a MinION Mk1C (1366 pores available). Sequencing was carried out for 44 h resulting in 1.57 M reads and 2.73 Gb raw data. Raw Nanopore reads were corrected using Canu version 2.2 [80] and used to perform a metaSPAdes hybrid assembly with the Illumina data. After binning the contigs with MetaWRAP, this again resulted in a Verstraetearchaeial bin (1.54Mb, 2 contigs). Additionally, corrected Nanopore reads were assembled using metaFlye version 2.9.1 [81]. This resulted in a Verstraetearchaeial single-contig of 1.43 Mb. This contig was corrected with the raw Illumina reads, in three rounds/iterations, using Pilon version 1.23 [82]. Analysis showed that the overlapping areas of the 5 contigs of the 3 Verstraetearchaeial bins were identical and could be combined into a single contig. To this end, raw Illumina reads were mapped onto the 5 contigs using Burrows-Wheeler Aligner (bwa, https://github.com/lh3/bwa) after which mapped reads were extracted from the original Illumina dataset. These reads were used in a SPAdes v3.14.0 assembly to which the 5 contigs were added under the flag *–trusted-contigs*. This gave a single circular contig (1538194 bp) of strain LWZ-6.

Phylogenomic and phylogenetic tree construction

To phylogenomically place the 5 representative MAGs, publicly available MAGs classified as *Ca*. Verstraetearchaeota, *Ca*. Culexarchaeia, *Ca*. Nezhaarchaeota and *Ca*. Methanomethylicia were downloaded from GTDB, JGI, and NCBI repositories, together with a set of 92 high-quality genomes spanning archaeal diversity. All MAGs were first analyzed with checkM2 (https://github.com/chklovski/CheckM2). MAGs with completeness below 60% and contamination above 10% were removed from the dataset. Subsequently, the proteomes of all remaining MAGs were predicted using Prodigal [83]. The phylogenomic tree was constructed using a set of 76 archaeal markers (Archaea76) [84]. To retrieve orthologues from the proteomes and create single marker alignments, GToTree was run with standard parameters. Maximum likelihood (ML) individual protein phylogenies were generated using IQ-TREE v2.0.3 [85] under the LG+C20+F+G substitution model with 1000 ultrafast bootstraps. Phylogenetic trees were manually inspected for erroneous inclusion of paralogous or contaminated sequences. If present, such sequences were removed from the dataset, after which remaining sequences were realigned, and phylogenies were re-estimated, as described above. The final single marker alignments were then concatenated into one. Columns with gaps in more than 90% of the sequences were removed using trimAl v1.4.rev22 [86], resulting in an alignment of 12084 positions. A first maximum likelihood (ML) phylogenetic tree was generated using IQ-TREE v2.0.3 [85] (-bb 1000 -alrt 1000) with the model LG+C60+F+G. The resulting ML tree was then used to generate a posterior mean site frequency ML tree (-tbe -b 100 flags).

Furthermore, a McrA gene phylogeny tree was constructed using 115 McrA sequences retrieved from the 6 representative Verstraetearchaeal MAGs and draft genomes from publicly available (potential) methanogenic taxa of the TACK superphylum, Euryarchaeota, and Helarchaeota. The sequences were first aligned using MAFFT v7.310 [87]. Columns with gaps in more than 10% of the sequences were removed using trimAl v1.4.rev22 [86]. The maximum likelihood (ML) phylogenetic tree was then generated using IQ-TREE v2.0.3 [85] (-bb 1000 -alrt 1000) with the model Q.pfam+C40+F+G8, as chosen by the Bayesian information criterion (BIC) using ModelFinder Plus [88]. The resulting ML tree was then used to generate a posterior mean site frequency ML tree (-tbe -b 100 flags).

Transcriptome sequencing and data analysis

Total RNA was extracted at the exponential methane production stage of strain LWZ-6 when Verstraetearchaeial culture was incubated with methanol and hydrogen in fresh medium. RNA was sent to Novogene for sequencing. The RNA-seq data was produced by NovaSeq6000 instrument with PE150 at Novogene (https://en.novogene.com). The raw data were first trimmed by removing the adaptors and low-quality sequences using Trimmomatic [67] and the mRNA was retrieved with SortMeRNA [89] with default settings after removal of tRNA and rRNA.

Evaluation of the activity of strain LWZ-6 was conducted using the complete circular LWZ-6 genome for analysis. The transcription of genes was calculated using Burrows-Wheeler Aligner (BWA, v. 0.7.17-r1188) [90]. The SAM mapping file was transformed into BAM files by SAMtools (v. 1.13) [91]. The read coverage

was calculated using BEDTools (v. 2.30.0) [92]. Numbers of reads was normalized to the length of the genome. Fragments per kilobase million (FPKM) were used to normalize the expression level. The transcribed rank of genes was calculated on $\log_2$[FPKM].

Screening 16S rRNA of Verstraetearchaeia in public databases

The 16S rRNA gene reference sequences extracted from the Verstraetearchaeia genomes were submitted to the Integrated Microbial Next Generation Sequencing (IMNGS) platform (https://www. imngs.org/). SRA sequences were retrieved using a similarity cutoff of 90% at a minimum length of 200 bp. 10774 sequences were obtained from IMNGS in which 5187 were present in a relative abundance of at least 0.1% in the dataset. These were grouped into 692 clusters with a 95% similarity cutoff using CD-HIT [93]. The Verstraetearchaeial reference sequences and the representative sequence of each CD-HIT cluster together with near-complete 16S rRNA gene sequences from other Archaea and Bacteria were aligned with MAFFT v7.310 [87]. This alignment was used to construct a phylogenetic tree using IQ-TREE v2.0.3 REF (-bb 1000 -alrt 1000) [85]. From this tree, CD-HIT cluster representative sequences robustly grouping with Verstraetearchaeales were linked back to the unclustered dataset of 5187 sequences. This resulted in 1091 sequences clustering with Verstraetearchaeales. The metadata from the sequencing datasets in which these sequences were found was used to analyze the global distribution of Verstraetearchaeales. World map shape with geographical coordinates of Verstraetearchaeales 16S rRNA gene sequences and genomes was created using ggmap [94].

Figures

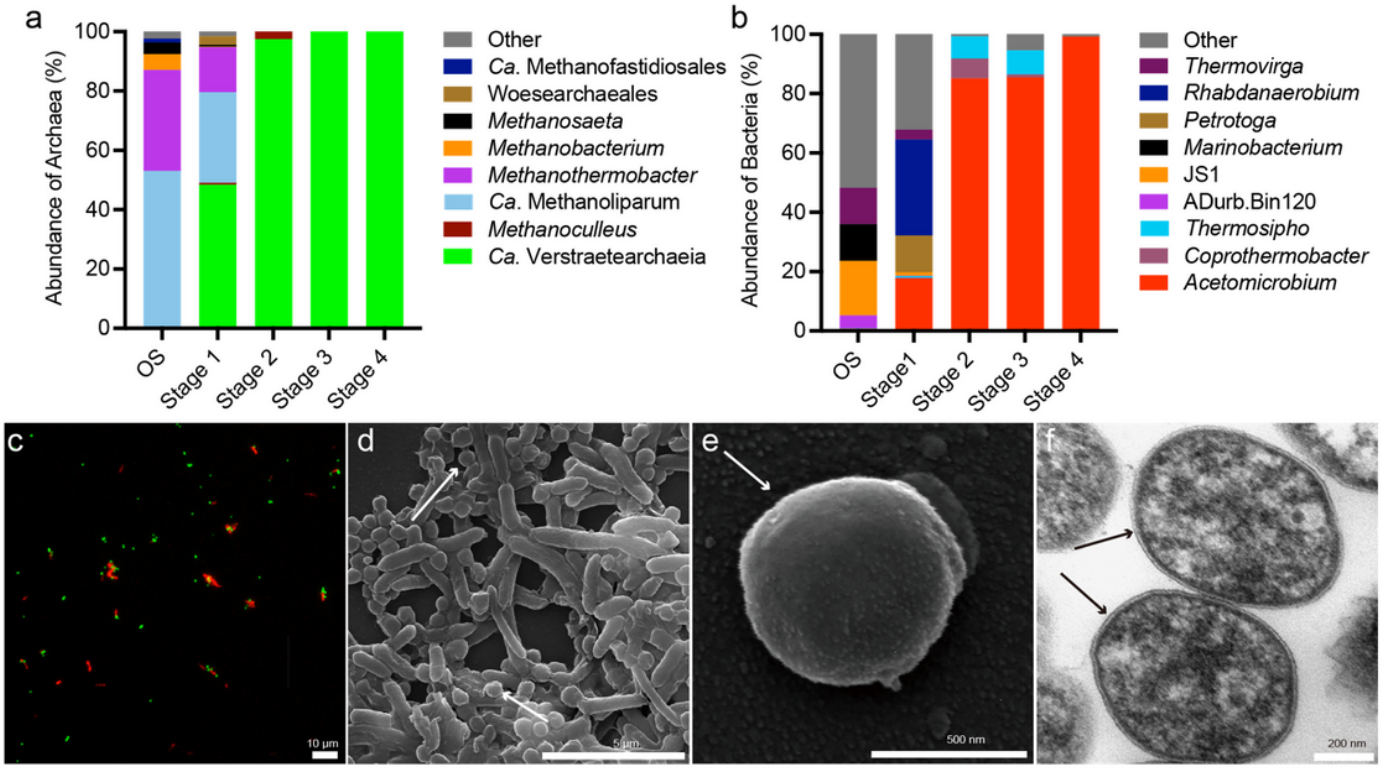

Figure 1

Isolation stages and microscopy observation of a Verstraetearchaeial co-culture. Comparison of archaeal (**a)** and bacterial (**b**) communities at the genus level in original samples (OS) and the 4 isolation stages. 16S rRNA gene amplicon sequencing was performed using archaeal and bacterial primers of 519F/915R [26] and 341F/806R [27], respectively. **c**, CARD-FISH images of cells from the co-culture. hybridized with nucleotide probes that target archaea ARCH-915 [26] (green) and EUB-338 [28] (red), **d**, **e**, SEM images of the co-culture, with white arrows indicating LWZ-6 cells. **f**, TEM showing ultrathin section of the coculture, black arrows indicate cells of LWZ-6. Scale bars: 10 µm (**c**), 5 µm (**d**), 500 nm (**e**), 200 nm (**f**).

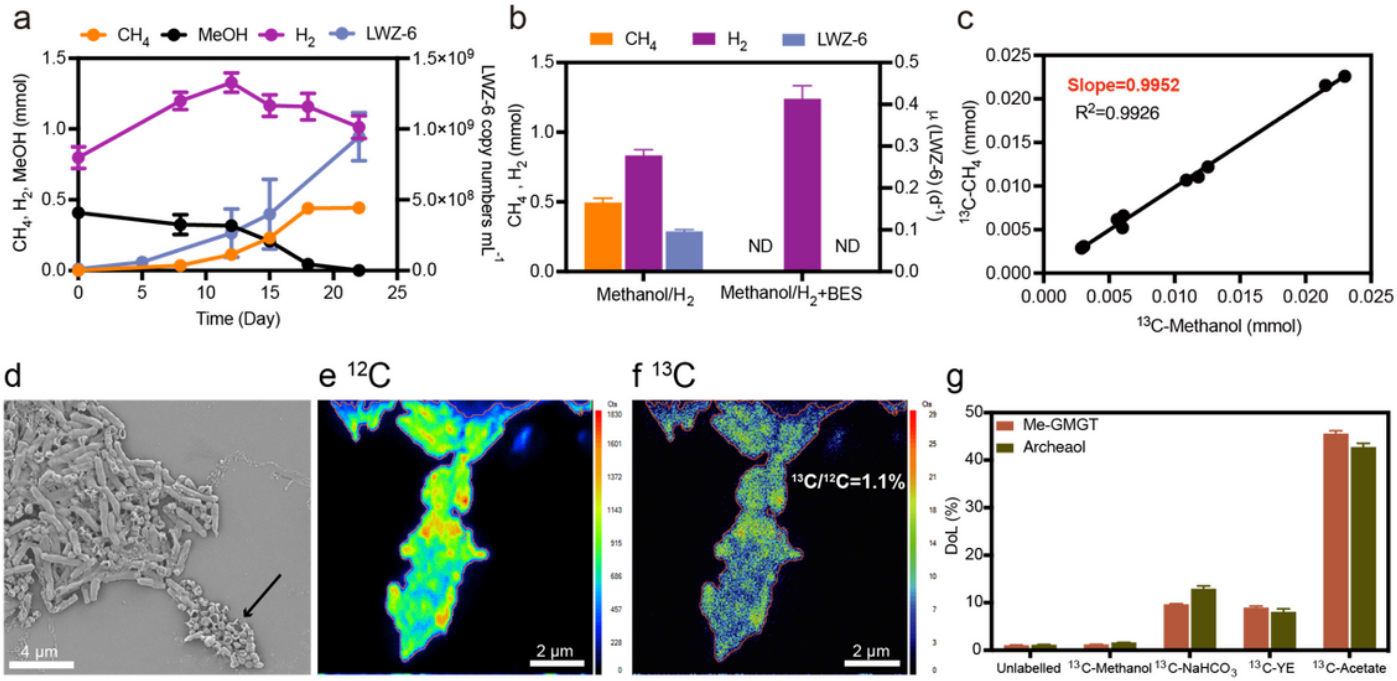

Figure 2

Growth dynamics and methanogenic activity of LWZ-6 a, Methanogenesis activity when the *V. methanopetracarbonis* LWZ-6/*Acetomicrobium* sp. CY-2 co-culture was incubated with methanol and hydrogen, **b**, Methane production by adding 2-bromoethanesulfonate (BES). ND: no methane detected. The methane and hydrogen were detected in the stationary phase. The co-culture was incubated in 50 mL fresh medium at 55 °C. Methanol: 10 mM methanol, BES: 10 mM BES, H_2: 10 kPa H_2, μ represents the specific growth rate of strain LWZ-6. **c**, Stable isotope tracer experiments elucidate ^{13}C-methane produced when supplemented with different ratios (1, 2, 4, 8%) of ^{13}C-methanol addition. **d**, SEM images prior to NanoSIMS targeting strain LWZ-6, the black arrow indicates strain LWZ-6. **e**, **f**, NanoSIMS ion images of ^{12}C and ^{13}C in strain LWZ-6 when incubated with labeled methanol, ^{13}C/^{12}C=1.1% shows the relative abundance in cells. **g**, Lipid-SIP showing the labeled archaeol and Me-GDGT-0 determined in strain LWZ-6 when the co-culture was incubated with labeled acetate, methanol, $NaHCO_3$, or yeast extract (YE), DoL represents the total degree of ^{13}C labeling lipids. The NanoSIMS analysis was conducted in triplicates. All symbols represent means of three individual incubations, error bars represent Standard Deviation (SD) of triplicates, the invisible error bars are the ones smaller than symbols.

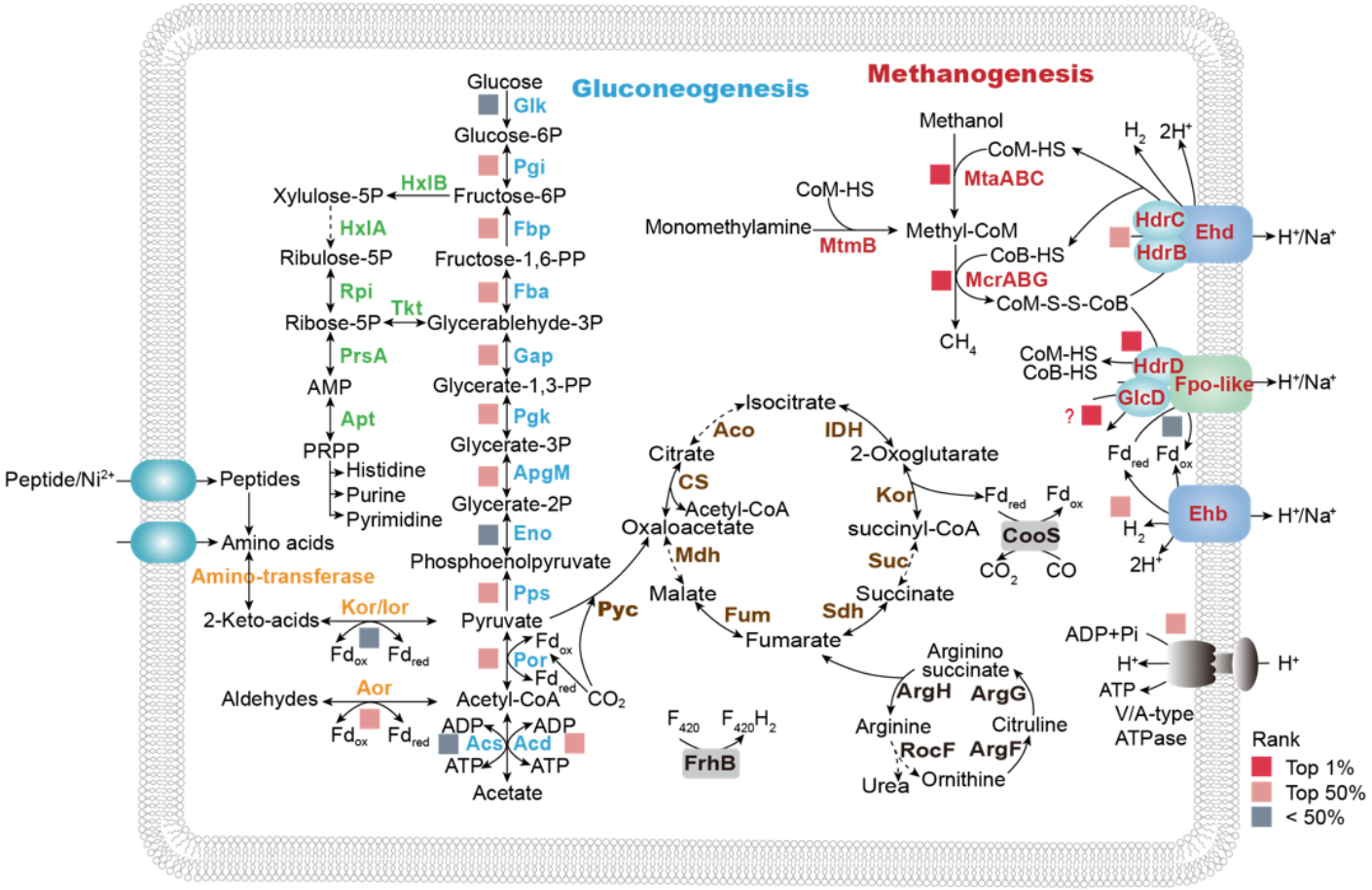

Figure 3

Reconstruction of the metabolic pathways of strain LWZ-6. The bold arrows indicate the identified genes in the complete circular genome, and the dotted line represents the genes not found in the genome. Proteins labelled in red, blue, green, orange, and brown are involved in methanogenesis, gluconeogenesis, the nucleotide salvage pathway, amino acids biosynthesis, and the TCA cycle. The transcriptome data of *V. methanopetracarbonis* LWZ-6 was collected at the log phase of methane production with the addition of methanol and hydrogen. The transcript abundance rank was based on the $\log_2$[FPKM] values as indicated by colored squares referenced to that at the right lower corner. The genes described in the figure and their abbreviations are presented in Supplementary table 2.

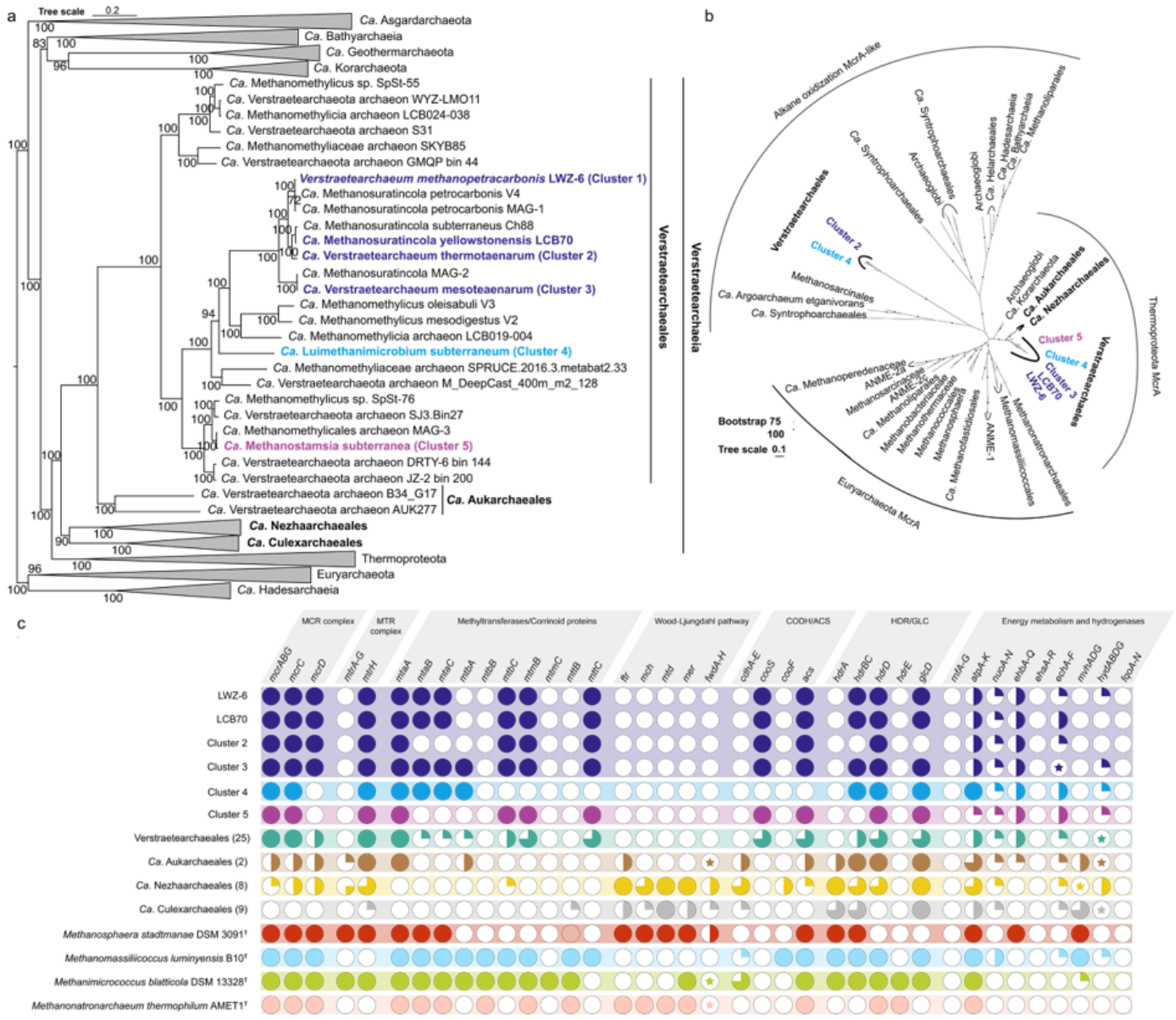

Figure 4

Phylogeny tree and methanogenic features of 5 Verstraetearchaeial species-level clusters in our study. a, Phylogenomic tree of 5 clusters from our enrichments (colored fonts) based on 76 archaeal marker genes using 127 genomes from available databases. The concatenated alignments were filtered with trimAl, after which a maximum likelihood (ML) tree was constructed using IQ-TREE (LG+C60+F+G model) with 100 nonparametric bootstrap replicates. The 5 species-level clusters are *Ca*. Verstraetearchaeum methanopetracarbonis (Cluster 1), *Ca*. V. thermotaenarum (Cluster 2), *Ca*. V. mesootaenarum (Cluster 3), *Ca*. Luimethanimicrobium subterraneum (Cluster 4), *Ca*. Methanostamsia subterranea (Cluster 5), of which 5 representative MAGs were chosen for analysis (Detailed information is presented in Supplementary Table 3). **b**, Phylogeny of methyl-coenzyme M reductase subunit A (McrA) of 5 clusters (colored fonts). The phylogenetic tree was constructed with 115 McrA sequences. Sequences were

aligned using MAFFT after which the alignment was trimmed with trimAl resulting in an alignment of 544 positions. The ML tree was generated using IQ-TREE (Q.pfam+C40+F+G8 model) with 100 nonparametric bootstrap replicates. **c**, Methanogenetic features of 5 Verstraetearchaeial clusters in our study in comparison other *Ca*. Verstraetearchaeales, *Ca*. Nezhaarchaeales, and *Ca*. Culexarchaeales genomes and Euryarchaeotal hydrogen-dependent methylotrophic methanogens. Circles indicate gene/gene sets identified (filled), gene/gene sets identified in at least 75% of MAGs (¾ filled), gene/gene sets identified in at least 50% of the MAGs (half filled), gene/gene sets identified in at least 25% of MAGs (¼ filled), gene/gene sets identified in less than 25% of MAGs (star), gene/gene sets not identified (open). The genes described in the figure and their abbreviations are listed in Supplementary Table 4.

Supplementary Files

This is a list of supplementary files associated with this preprint. Click to download.

- SupplementaryTable.xlsx
- SupplementaryInformation.docx
- ExtendedData.docx